

See discussions, stats, and author profiles for this publication at: <https://www.researchgate.net/publication/8067516>

Folding, Stability and Polymerization Properties of FtsZ Chimeras with Inserted Tubulin Loops Involved in the Interaction with the Cytosolic Chaperonin CCT and in Microtubule Forma...

ARTICLE *in* JOURNAL OF MOLECULAR BIOLOGY · MARCH 2005

Impact Factor: 4.33 · DOI: 10.1016/j.jmb.2004.11.054 · Source: PubMed

CITATIONS

9

READS

43

6 AUTHORS, INCLUDING:



Isabel Barthelemy

Spanish National Centre for Cardiovascular...

20 PUBLICATIONS 456 CITATIONS

SEE PROFILE



Marian Oliva

Centro de Investigaciones Biológicas

12 PUBLICATIONS 572 CITATIONS

SEE PROFILE



José L Carrascosa

Spanish National Research Council

290 PUBLICATIONS 7,840 CITATIONS

SEE PROFILE



Jose Manuel Andreu

Centro de Investigaciones Biológicas

166 PUBLICATIONS 5,742 CITATIONS

SEE PROFILE

Folding, Stability and Polymerization Properties of FtsZ Chimeras with Inserted Tubulin Loops Involved in the Interaction with the Cytosolic Chaperonin CCT and in Microtubule Formation

Sara Bertrand¹, Isabel Barthelemy¹, María A. Oliva², José L. Carrascosa¹
José M. Andreu² and José M. Valpuesta^{1*}

¹Centro Nacional de Biotecnología, C.S.I.C. Campus de la Universidad Autónoma de Madrid, 28049 Madrid, Spain

²Centro de Investigaciones Biológicas, C.S.I.C. Ramiro de Maeztu 9, 28040 Madrid Spain

To attain its native conformation, the cytoskeletal protein tubulin needs the concurrence of several molecular chaperones, among others the cytosolic chaperonin CCT. It has been previously described that denatured tubulin interacts with CCT in a quasi-folded conformation using several loops located throughout its sequence. These loops are also involved in microtubule formation and are absent in its prokaryote homologue FtsZ, which *in vitro* folds by itself and does not interact with CCT. Several FtsZ/tubulin chimeric proteins were generated by inserting consecutively one, two or three of the CCT-binding domains of tubulin into the corresponding sequence of FtsZ from *Methanococcus jannaschii*. The insertion of any of the CCT-binding loops generates in the FtsZ/tubulin chimeras the ability to interact with CCT. The accumulation of CCT-binding loops induces in the FtsZ/tubulin chimeras unfolding and refolding properties that are more similar to tubulin than to its prokaryote counterpart. Finally, the insertion of some of these loops generates in the FtsZ/tubulin chimeras more complex polymeric structures than those found for FtsZ. These results reinforce the notion that CCT has coevolved with tubulin to deal with the folding problems encountered by the eukaryotic protein with the appearance of the new sequences involved in microtubule formation.

© 2004 Elsevier Ltd. All rights reserved.

*Corresponding author

Keywords: tubulin; FtsZ; chaperonin; protein folding; electron microscopy

Introduction

Microtubules, like other cytoskeletal structures, are critical for the survival of eukaryotes, since they are involved not only in the maintenance of the cell shape, but also in cell motility, cell transport and mitosis.¹ Microtubules are cylindrical polymers composed of parallel protofilaments, each one made up of heterodimers of the very homologous α - and β -tubulin. Tubulins are unique to eukaryotes, with the exception of the bacterial genus *Prostheco bacter*,² and have a complex folding pathway that is controlled by a set of molecular chaperones,^{3,4} among others the eukaryotic

chaperonin CCT (chaperonin containing TCP-1; also termed c-cpn or Tric^{5–7}). CCT shares similar structural features with the rest of the chaperonins, a double-ring toroidal oligomer with each monomer having a three-domain structure: the equatorial domain holding the nucleotide binding site and most of the intra- and inter-ring interactions, an intermediate domain that acts as a transmitter of the signals between the equatorial and the apical domain, which holds the substrate binding domain. CCT also cycles between an open, nucleotide-free conformation that recognizes and binds the unfolded substrates, and a closed, nucleotide-bound conformation where folding takes place.^{8,9} However, there are important differences between CCT and the rest of the chaperonins. CCT is by far the most complex of all known chaperonins, since it is composed of eight different, albeit homologous subunits, positioned in a precise arrangement within the chaperonin ring,^{10,11} which suggests a

Abbreviations used: CCT, chaperonin containing TCP-1; GdmCl, guanidinium chloride.

E-mail address of the corresponding author: jmv@cnb.uam.es

specificity in the interaction between the cytosolic chaperonins and their substrates. CCT, unlike other chaperonins, seems to act over a broad but defined set of substrates, using a different mechanism than that described for GroEL, which has been studied mainly for the two major substrates, the cytoskeletal proteins actin and tubulin.^{12,13} This mechanism involves binding of the unfolded protein in the open, substrate-receptive conformation, and its folding using the conformational changes that undergo the cytosolic chaperonin upon nucleotide binding.¹⁴

The interaction with CCT is stringent for the folding of tubulin^{15,16} and occurs through a mechanism that involves the interaction of specific subunits of the chaperonin with specific regions of a tubulin molecule that has already acquired a large degree of conformation.^{9,17} The CCT-binding domains of tubulin, described by both biochemical and biophysical techniques, are located throughout its sequence^{17,18} and correspond to loops that are also involved in microtubule formation.^{17,19,20} Most of these loops are absent in the prokaryote

homologue of tubulin, FtsZ,²¹ which does not require the help of chaperones for its proper folding.²⁰ FtsZ is involved in cytokinesis and is the main component of the cell division machinery.²² However, the polymers generated by FtsZ are less complex than those formed by tubulin.²³ Being the structural core of the two cytoskeletal proteins very similar,^{21,24} it has been suggested that the extra regions in the eukaryotic protein have originated as a consequence of the evolution of tubulin from a prokaryote ancestor,¹⁷ providing the former protein with more powerful polymerising properties that are so critical in the function of eukaryotes. To investigate the role of these loops in the interaction with CCT and to characterise their polymerising properties, some of these sequences have been inserted into the corresponding regions of the homologous FtsZ from *Methanococcus jannaschii*. Whereas the various FtsZ/tubulin chimeras express as soluble proteins and their secondary structures are similar to that of wild-type FtsZ, the unfolding/folding analyses point to an increase of instability and a more elaborate folding

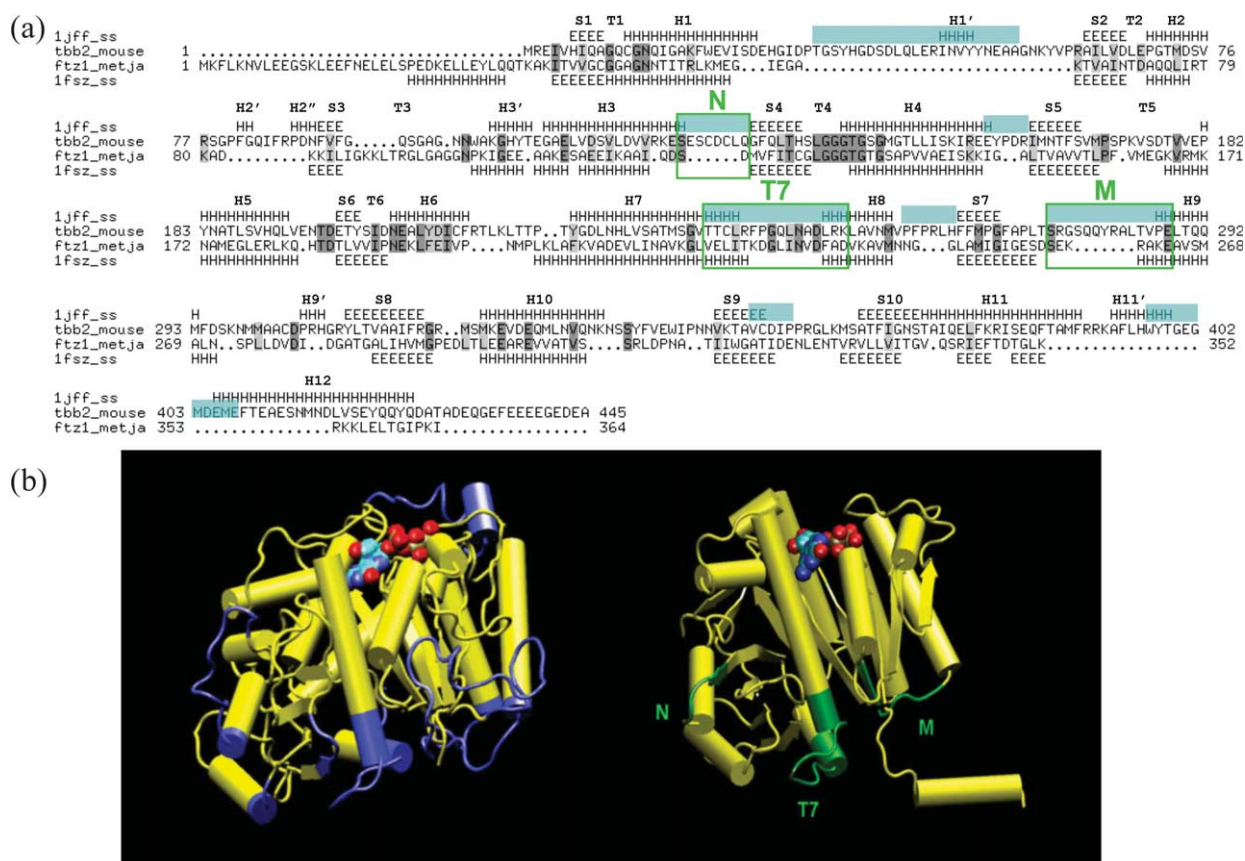


Figure 1. Tubulin domains involved in CCT interaction and microtubule formation. (a) Structure-based alignment of the sequences of the major brain β 2-tubulin isotype from mouse⁴¹ (*Mus musculus*) (tbb2_mouse; GeneBank accession NP033476) and cell division protein FtsZ from *Methanococcus jannaschii*²¹ (fts2_metja). The secondary structures of tubulin from pig brain (PDB entry 1JFF) and FtsZ from *M. jannaschii* (PDB entry 1FSZ), are also depicted in the alignment (E, β -sheet; H, α -helix). The CCT-binding loops of the tubulin sequence are marked blue. The three tubulin CCT-binding motifs chosen for substitution into the FtsZ sequence of *M. jannaschii* are boxed and termed N, T7 and M. (b) Three-dimensional structures of β -tubulin (left) and FtsZ from *M. jannaschii* (right). In the tubulin structure, the blue domains are those involved in CCT interaction. In the FtsZ structure, the three green regions are those where the N, T7 and M loops of tubulin have been inserted.

process that seems to be related to the number of loops inserted in the FtsZ sequence. The CCT binding assays reveal that the sequences inserted in FtsZ are indeed involved in the interaction of tubulin with the cytosolic chaperonin, and the polymerisation experiments carried out with the FtsZ/tubulin chimeras show that the polymers generated are different from those produced by wild-type FtsZ and more compatible with the lateral distortions introduced by the exogenous tubulin sequences.

Results

The generation of FtsZ/tubulin chimeras

Although FtsZ and tubulin share similar structure (Figure 1), they also have important differences in their folding and polymerising properties. Whereas FtsZ is able to fold by itself *in vitro* and may not need the help of any chaperone *in vivo*, tubulin needs the help of a set of chaperones to attain its functional conformation. Among others, the interaction with CCT is stringent for the proper folding of tubulin. The three-dimensional reconstruction carried out by electron microscopy of the complex between CCT and unfolded tubulin reveals that tubulin interacts with the cytosolic chaperonin after having acquired a certain conformation.⁹ Docking of the atomic conformation of tubulin into the tubulin mass of the CCT:tubulin complex reveals that the cytoskeletal protein seems to interact with CCT through a defined set of loops distributed throughout its sequence¹⁷ (Figure 1(a)). Most of these loops have been confirmed by biochemical experiments with synthetic peptides to be CCT binders¹⁸ and, when analysed in a comparison between FtsZ and tubulin sequences, they are absent in the prokaryote homologue^{17,20} (Figure 1(a)). These loops seem to be not only involved in the interaction with CCT but also in the formation of the microtubule,^{19,20} a more complex polymer than that generated by FtsZ. We chose three of these domains to study their CCT-binding and polymerising properties and for that, we introduced them in the corresponding region of FtsZ (Figure 1). The first one was a loop located in the N-terminal domain of the tubulin sequence, between α -helix 3 (H3) and β -strand 4 (S4), here called the N-loop, involved in both longitudinal and lateral contacts in the microtubule formation.¹⁹ The chimera generated, FtsZ/N, had the sequence S₁₂₃D of *M. jannaschii* switched by the sequence S₁₂₆ESCDCLQ of mouse β -tubulin. The second sequence mutated corresponded to the so-called T7-loop, located in the C-terminal domain of the tubulin sequence, between α -helices H7 and H8. Although this loop is conserved among all the FtsZ and tubulin sequences, it is very important in the longitudinal contacts along the protofilaments and for the GTPase activity of the dimer,^{19,25} and we decided to switch the T7 loop of FtsZ of *M. jannaschii* V₂₂₃ELITKDGLINVDFAD by that

of β -tubulin T₂₃₄TCLRFPGQLNADLRK, thus generating the FtsZ/T7 chimera, which should have a non-hydrolysable nucleotide due to the substitution of the essential D₂₃₈ by K.^{19,25} The third region chosen was that of tubulin M-loop (for microtubule formation), located between S7 and H9, which is very important in the generation of lateral contacts in the microtubule¹⁹ and in the interaction with CCT.^{9,17,18,26–28} This chimera, termed FtsZ/M, was generated by switching the FtsZ sequence S₂₅₈EKRAKE by the corresponding β -tubulin sequence S₂₇₇RGSQQYRALTVPE. A fourth chimera, FtsZ/T7M, was generated by accumulating the insertions produced in the FtsZ/T7 and FtsZ/M chimeras. Finally, a fifth mutant, FtsZ/NT7M was generated by adding the insertions produced in the FtsZ/N, FtsZ/T7 and FtsZ/M chimeras.

Folding of the FtsZ/tubulin chimeras

The FtsZ/tubulin chimeras were cloned in *Escherichia coli* and all five mutants were expressed as soluble proteins. However, FtsZ/N was expressed in small amounts, which prevented us from performing any analysis demanding substantial amounts of protein, such as the circular unfolding/folding experiments described below. Surprisingly, the triple mutant FtsZ/NT7M, which also contains the N-loop insertion, posed no problem in generating enough protein, although in this case, approximately half of the expressed protein was in the form of insoluble aggregates.

The purified FtsZ/T7, FtsZ/M, FtsZ/T7M and FtsZ/NT7M chimeras were subjected to circular dichroism (CD) analysis, and their spectra were found to be similar to that of wild-type FtsZ (Figure 2(a)). From these measurements we concluded that the average secondary structure of FtsZ, as monitored by CD, is not significantly perturbed by the insertion of the tubulin loops. In addition, all four mutants contained bound guanine nucleotide as did wild-type FtsZ (see Materials and Methods). All this supports the notion that the chimeras are correctly folded in *E. coli*, similarly to FtsZ.

In order to examine the stability and the spontaneous folding ability of the purified FtsZ/tubulin chimeras, their equilibrium unfolding/refolding curves were determined by measuring the change in CD at 222 nm as a function of GdmCl concentration (Figure 2(b)–(e)). FtsZ/T7 unfolding was completely reversible, although this construct was significantly less stable to GdmCl than FtsZ (Figure 2(b); the denaturant concentrations for half-unfolding were 1.9 M and 3.1 M GdmCl, respectively). FtsZ/M also had a reversible unfolding profile (Figure 2(c); midpoint 2.6 M GdmCl), although in this case more similar to that of FtsZ than that of FtsZ/T7. The FtsZ/T7M chimera unfolded reversibly, but with a biphasic profile (Figure 2(d), with approximate midpoints 1.3 M and 2.3 M GdmCl; the CD spectrum of refolded FtsZ/T7M coincided with that of the native protein

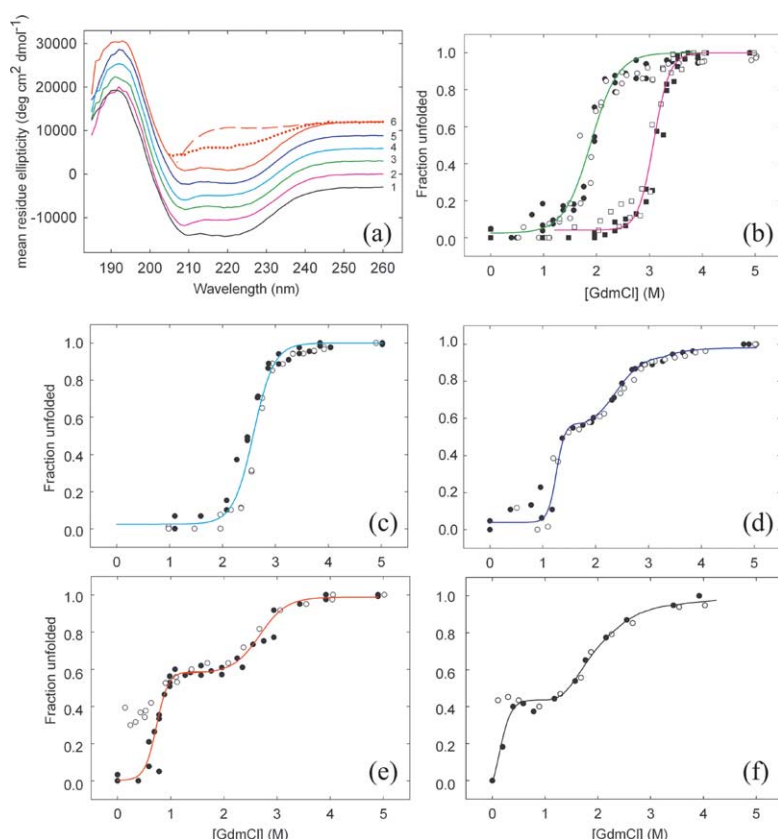


Figure 2. Secondary structure unfolding and folding behaviour of the FtsZ chimeras. (a) Circular dichroism spectra of FtsZ/tubulin chimera. Line 1, tubulin (Andreu *et al.*²⁰); line 2, FtsZ; line 3, FtsZ/T7 chimera; line 4, FtsZ/M chimera; line 5, FtsZ//T7M chimera; continuous line 6, FtsZ/NT7M chimera. Each of these spectra is an average from two separate protein preparations, in 20 mM Tris-HCl (pH 7.9) at 25 °C; the lines have been shifted by 3000 units in the Y-axis in order to distinguish them. Broken lines 6, FtsZ/NT7M in 6 M GdmCl. Dotted line 6, a FtsZ/NT7M sample in which the denaturant had been diluted from 6 M to 0.6 M GdmCl (see also (e)). (b)–(e) GdmCl unfolding/refolding curves of FtsZ/tubulin chimeras (0.16 mg/ml) in 20 mM Pipes-KOH (pH 7.5) at 25 °C. The fraction of unfolded protein was calculated from the change in circular dichroism at 222 nm and plotted against the denaturant concentration. Filled symbols, increasing GdmCl concentrations. Open symbols, decreasing GdmCl

concentrations obtained by dilution from 6 M GdmCl. Each set of data comes from three separate experiments. (b) Squares, wild-type FtsZ; circles, FtsZ/T7 chimera, placed together for comparison. (c) FtsZ/M chimera. (d) FtsZ/T7M chimera. (e) FtsZ/NT7M chimera. (f) Tubulin (Andreu *et al.*²⁰). The continuous lines in (b) and (c) are two-state model fits³⁸ to the collected data with half denaturant concentrations 3.1 M GdmCl (FtsZ), 1.9 M GdmCl (FtsZ/T7) and 2.6 M GdmCl (FtsZ/M), and unfolding free energy changes 12.3 Kcal mol^{−1} (FtsZ), 4.4 Kcal mol^{−1} (FtsZ/T7) and 7.9 Kcal mol^{−1} (FtsZ/M). The continuous lines in (d), (e) and (f) are arbitrary double sigmoid lines simply drawn to show the trend of the data in these multi-stage transitions, which have identifiable half denaturant concentrations at approximately 1.2 M and 2.3 M GdmCl (FtsZ/T7M chimera), and 0.7 M and 2.7 M GdmCl (FtsZ/NT7M chimera), and 0.2 M and 2 M GdmCl (tubulin).

(not shown)). The FtsZ/NT7M chimera showed also a biphasic unfolding profile (Figure 2(e), with approximate midpoints 0.7 M and 2.7 M GdmCl), similar to that of tubulin $\alpha\beta$ dimers (Figure 2(f)), and as in the case of the eukaryotic protein, this triple mutant failed to refold completely upon dilution of GdmCl (compare in both Figure 2(e) and (f) the unfolding data (filled circles) with the refolding profile (open circles)). The CD spectrum of FtsZ/NT7M from which the denaturant had been diluted (Figure 2(a), dotted line 6) was clearly different from the spectrum of either the native or the fully unfolded FtsZ/NT7M (Figure 2(a), continuous lines and broken lines 6, respectively). Employing a tenfold lower protein concentration, or diluting the denaturant in the cold did not improve the partial refolding of FtsZ/NT7M. These results indicate that insertion of the M, and T7 loops into FtsZ progressively reduces stability of FtsZ, and that further insertion of the N-loop increases the complexity of the folding process, to the point of hampering spontaneous *in vitro* refolding of the FtsZ/NT7M chimera.

The interaction of the FtsZ/tubulin chimeras with the cytosolic chaperonin CCT

As discussed above, the three loops inserted in the FtsZ sequence are involved in the interaction of tubulin with the cytosolic chaperonin CCT,¹⁷ so in order to qualitatively determine whether these domains were capable of providing FtsZ with the ability to interact with the chaperonin, we performed a CCT binding assay with the FtsZ/tubulin chimeras (Figure 3). The different proteins were incubated with CCT and the putative complexes run on a native gel. The band corresponding to CCT was excised and loaded onto an SDS gel (Figure 3(a)) and subsequently immunoblotted with antibodies against tubulin or FtsZ (Figure 3(b)). Two controls were included to confirm the validity of the technique. As a positive control of the interaction of the chaperonin with unfolded substrate, chemically unfolded tubulin was diluted in the presence of CCT and the SDS gel revealed the presence of a band assigned to tubulin, either by N-terminal sequencing or with the use of a specific antibody

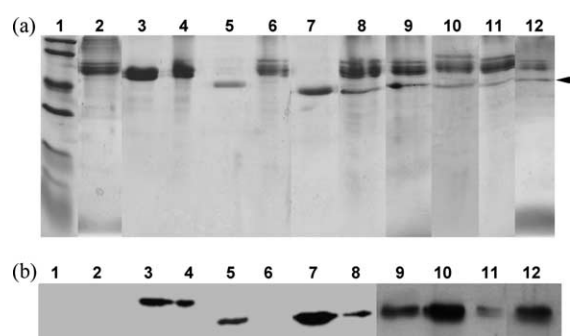


Figure 3. CCT binding assays of the FtsZ chimeras. (a) SDS-PAGE gel, and (b) immunoblot of the following samples. Lane 1, Molecular mass markers (94, 67, 43, 30, 20 and 14 kDa). Lane 2, CCT. Lane 3, β -tubulin. Lane 4, CCT incubated with unfolded β -tubulin. Lane 5, wild-type FtsZ. Lane 6, CCT incubated with unfolded FtsZ. Lane 7, FtsZ/M chimera. Lane 8, CCT incubated with unfolded FtsZ/N chimera. Lane 9, CCT incubated with unfolded FtsZ/T7 chimera. Lane 10, CCT incubated with unfolded FtsZ/M chimera. Lane 11, CCT incubated with unfolded FtsZ/T7M chimera. Lane 12, CCT incubated with unfolded FtsZ/NT7M chimera. As described in Materials and Methods, the various samples of unfolded proteins were incubated with CCT and run on a native gel. In the case of lanes 4, 6 and 8–11, the band corresponding to CCT was excised and the protein extracted and subsequently run on a SDS gel to detect the presence or absence of any protein bound to CCT, either visually (a) or with the help of specific antibodies (b). Arrowhead points to the FtsZ proteins.

against the eukaryotic protein (Figure 3 (b), lane 4). On the other hand and as a negative control, we performed the same kind of assay with unfolded wild-type FtsZ and found that it did not bind to CCT (Figure 3, lane 6). However, the same CCT binding assay performed with the five unfolded FtsZ chimeras revealed that they all interacted with CCT (Figure 3, lanes 8–12). This result confirms that the three tubulin domains are indeed involved in the interaction with the cytosolic chaperonin. The same CCT binding experiments were performed with native proteins, and whereas native tubulin or FtsZ did not bind to CCT, all five FtsZ chimeras maintained their CCT-binding ability (results not shown). These results together with those obtained

from the unfolding/folding experiments suggest that the unfolded FtsZ chimeras FtsZ/T7, FtsZ/M and FtsZ/T7M, when diluted in the presence of CCT to decrease the denaturant concentration, attain their native conformation before interacting with the cytosolic chaperonin.

The interaction between the FtsZ chimeras and CCT was examined in more detail using electron microscopy and image processing. This technique has been previously used to characterise the interaction between unfolded tubulin and CCT,⁹ and this study has revealed that the interaction occurred through two modes of binding of an open, quasi-folded conformation of tubulin with two opposite sides of the chaperonin cavity (see Figure 4(a)). We repeated this type of experiment here, and the various FtsZ/tubulin chimeras were unfolded, diluted in the presence of CCT, and a few hundreds particles of the CCT:FtsZ complexes obtained by electron microscopy were selected, processed and averaged. The average images obtained in all cases showed the mass of FtsZ not crossing the CCT cavity, as it is the case of the unfolded tubulin (Figure 4(a)), but interacting with one side of the chaperonin cavity (Figure 4(b) shows the average image of the CCT:FtsZ/M complex, but those of the other CCT:FtsZ complexes were similar). The same kind of experiment was carried out with CCT and the native FtsZ/tubulin chimeras, and the result was similar, with the FtsZ mass interacting with 2–3 subunits of the same side of the chaperonin cavity (Figure 4(c) shows the average image of the complex formed between CCT and native FtsZ/M chimera, but the average images of the complexes between CCT and any of the other folded FtsZ/tubulin chimeras were similar). These results confirm that the tubulin sequences inserted in the FtsZ structure provide the prokaryotic protein with the ability to interact with CCT.

As stated above, the interaction between CCT and unfolded tubulin involves specific domains of tubulin with defined CCT subunits. This was clearly determined by immunomicroscopy of CCT:tubulin complexes and monoclonal antibodies against specific CCT subunits,⁹ which showed that binding between the cytosolic chaperonin and the unfolded tubulin occurs through two modes of interaction, with the N-terminal domain of tubulin interacting

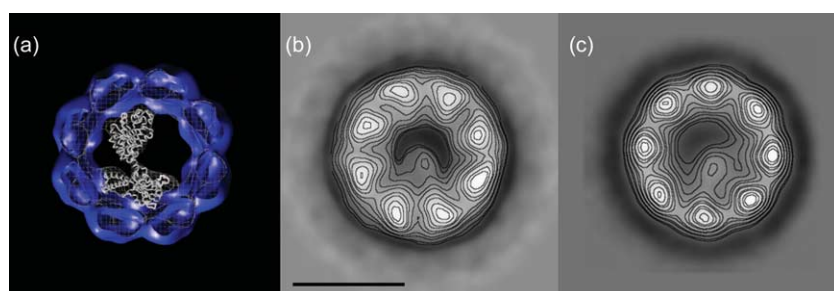


Figure 4. Two-dimensional average images of CCT:FtsZ complexes. (a) Mode of interaction between CCT and tubulin, according to the three-dimensional reconstruction of the CCT:tubulin complex and the docking of an open tubulin structure into the tubulin mass of the CCT:tubulin complex described by Llorca *et al.*⁹ (b) Average image of the complex formed by CCT and the unfolded FtsZ/M chimera (average of 485 particles). (c) Average image of the complex formed by CCT and the native FtsZ/M chimera (average of 581 particles). The bar in (b) represents 10 nm.

the unfolded FtsZ/M chimera (average of 485 particles). (c) Average image of the complex formed by CCT and the native FtsZ/M chimera (average of 581 particles). The bar in (b) represents 10 nm.

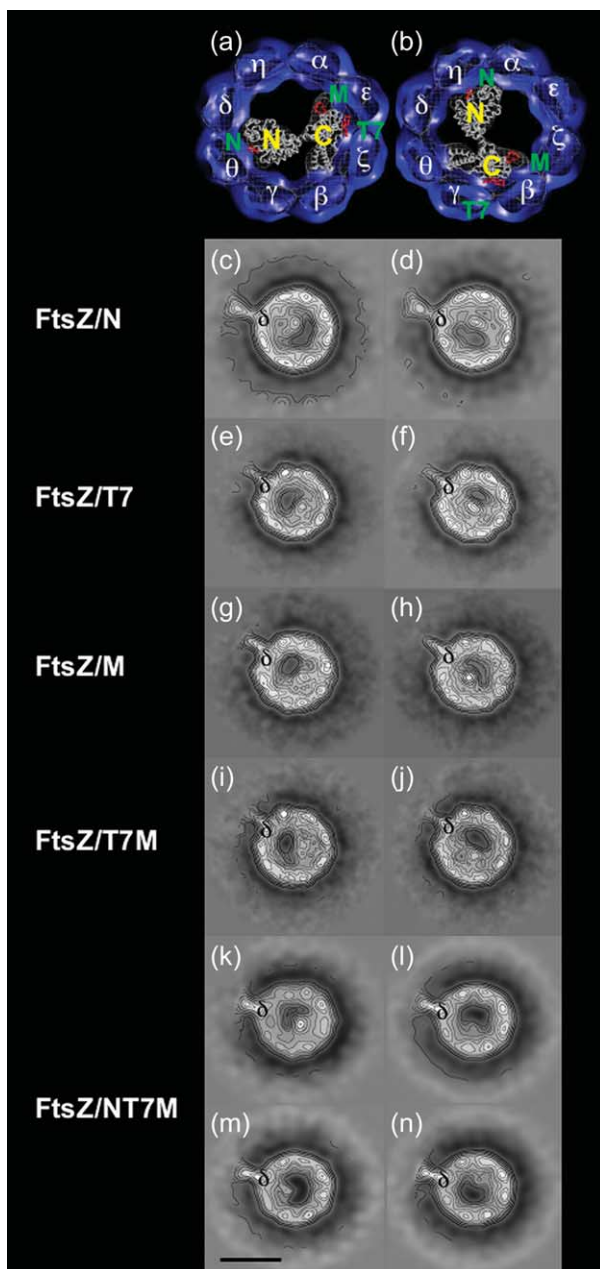


Figure 5. Two-dimensional average images of immunocomplexes of CCT:FtsZ with anti CCT δ antibody. (a) and (b) The two possible modes of interaction between CCT and tubulin, according to the three-dimensional reconstruction of the CCT:tubulin complex, the docking of an open tubulin structure into the tubulin mass of the CCT:tubulin complex, and the immunomicroscopy experiments described by Llorca *et al.*⁹ The topology of CCT subunits drawn in (a) is the one described by Liou *et al.*¹⁰ The red regions in the tubulin sequence both in (a) and (b) indicate the three loops (N-loop, T7-loop and M-loop) used for the generation of the FtsZ/tubulin chimeras. These domains are marked in green letters whereas the yellow letters mark the N and C-terminal domains of tubulin. (c) and (d) Average images of the complex between CCT and denatured FtsZ/N chimera (averages of 234 and 245 particles, respectively). (e) and (f) Average images of the complex between CCT and denatured FtsZ/T7 chimera (averages of 315 and 275 particles, respectively). (g) and (h) Average images of the complex between CCT and denatured FtsZ/M chimera

with CCT θ/δ (Figure 5(a)) or with CCT η/α (Figure 5(b)), and the C-terminal domain interacting with CCT $\epsilon/\zeta/\beta$ (Figure 5(a)), or with CCT $\beta/\gamma/\theta$ (Figure 5(b)). We wanted to examine whether the specificity of the interaction of tubulin with CCT was maintained with the CCT-binding domains inserted in the FtsZ mutants, and we incubated the complexes made with CCT and the five FtsZ/tubulin chimeras with a monoclonal antibody that reacts specifically against CCT δ .²⁹ In each case, several hundred particles of each of the immunocomplexes formed were selected, classified and averaged. In the case of the complex formed with CCT and the unfolded FtsZ/N chimera, two populations were obtained that rendered two different average images, one of them with the FtsZ mass apparently interacting with CCT $\theta/\delta/\eta$ (Figure 5(c)) and the other with FtsZ interacting with CCT $\eta/\alpha/\epsilon$ (Figure 5(d)). Although these average images are of low resolution, they reveal that the insertion of the N-loop, located in the N-terminal domain of tubulin, induces the interaction of FtsZ/N with similar CCT subunits as in the case of the tubulin N-terminal domain.⁹ The other two tubulin loops inserted in FtsZ (T7 and M-loop) are located in the C-terminal sequence of tubulin, and the image processing of immunocomplexes formed with CCT, the monoclonal antibody against CCT δ , and unfolded FtsZ/tubulin chimeras generated with the insertion of those tubulin loops (FtsZ/T7, FtsZ/M and FtsZ/T7M), produced in each case two different average images representing two different populations. In one case, the average image of the CCT:FtsZ/T7, CCT:FtsZ/M and CCT:FtsZ/T7M complexes showed the mass attributed to FtsZ interacting approximately with CCT $\epsilon/\zeta/\beta/\gamma$ (Figure 5(e), (g) and (i), respectively), whereas in the other case the FtsZ mass seemed to approximately interact with CCT $\zeta/\beta/\gamma/\theta$ (Figure 5(f), (h) and (j), respectively). These results also point to the T7 and M-loops as inducing the interaction of the FtsZ/T7, FtsZ/M and FtsZ/T7M chimeras with the same side of the CCT cavity as it has been shown to interact in the C-terminal region of the unfolded tubulin⁹ (Figure 5(a) and (b)). Finally, the FtsZ/NT7M chimera carries the insertion of three tubulin sequences, one belonging to the N-terminal domain (N-loop) and two the C-terminal domain (T7 and M-loops), and the classification of the immunocomplexes formed by CCT, the unfolded FtsZ/NT7M chimera and the monoclonal antibody against CCT δ generated four different populations, each one producing a different average image (Figure 5(k)–(n)). The two largest populations

(averages of 514 and 507 particles, respectively). (i) and (j) Average images of the complex between CCT and denatured FtsZ/T7M chimera (averages of 572 and 635 particles, respectively). (k)–(n) Average images of the complex between CCT and denatured FtsZ/NT7M chimera (averages of 353, 342, 148 and 133 particles, respectively). Bar (m) corresponds to 10 nm.

(representing in each case $\sim 35\%$ of the particles) gave rise to two average images with the FtsZ mass interacting approximately with either CCT $\epsilon/\zeta/\beta$ (Figure 5(k)), or with CCT $\beta/\gamma/\theta$ (Figure 5(l)), and according to the results described above suggest that these two types of interaction have been induced by the tubulin C-terminal sequences T7 and M-loop. The other two average images (representing in each case 15% of the particles) showed the FtsZ mass interacting approximately with either CCT θ/δ (Figure 5(m)), or with CCT $\eta/\alpha/\epsilon$ (Figure 5(n)), and point to these two types of interaction as induced by the tubulin N-terminal sequence N-loop. In all, the immunomicroscopy results shown here clearly confirm that the three tubulin sequences chosen in this work are involved in a specific interaction with certain CCT subunits,^{9,17,18} and that this role has been transmitted to the FtsZ/tubulin chimeras generated with the insertion of these tubulin sequences. This ability of the FtsZ/tubulin chimeras to interact with specific regions of CCT is not dependent on the chimeras being in an unfolded state, since immunomicroscopy experiments carried out with complex formed between CCT and the native chimeras produced in each case similar results as shown in Figure 5(c)–(n) (results not shown).

The formation of polymers with FtsZ/tubulin chimeras

It has been shown that, whereas tubulin protofilaments generate extended lateral interactions that give rise to microtubules, the primary assembly product of FtsZ has been described as a double-stranded filament made of two tubulin-like straight protofilaments, with lateral contacts different from those described for the microtubules.²³ Since it has been proposed that the CCT-binding domains of tubulin are also involved in the formation of microtubules,¹⁷ we wanted to know if the tubulin sequences inserted in the FtsZ structure were capable of mimicking any of the polymerising properties of tubulin. The polymers generated by the FtsZ/tubulin chimeras under the standard FtsZ assembly conditions (see Materials and Methods) were observed by negative-stain electron microscopy (Figure 6), which revealed qualitative differences with respect to those formed by wild-type FtsZ (Figure 6(a)). These included tube-like structures in the case of the polymers of the FtsZ/T7 chimera (Figure 6(b)), and curved filaments making up the different twisted polymers of FtsZ/M (Figure 6(c)), FtsZ/T7M (Figure 6(d)) and FtsZ/NT7M (Figure 6(f)) chimeras, as well as laminar

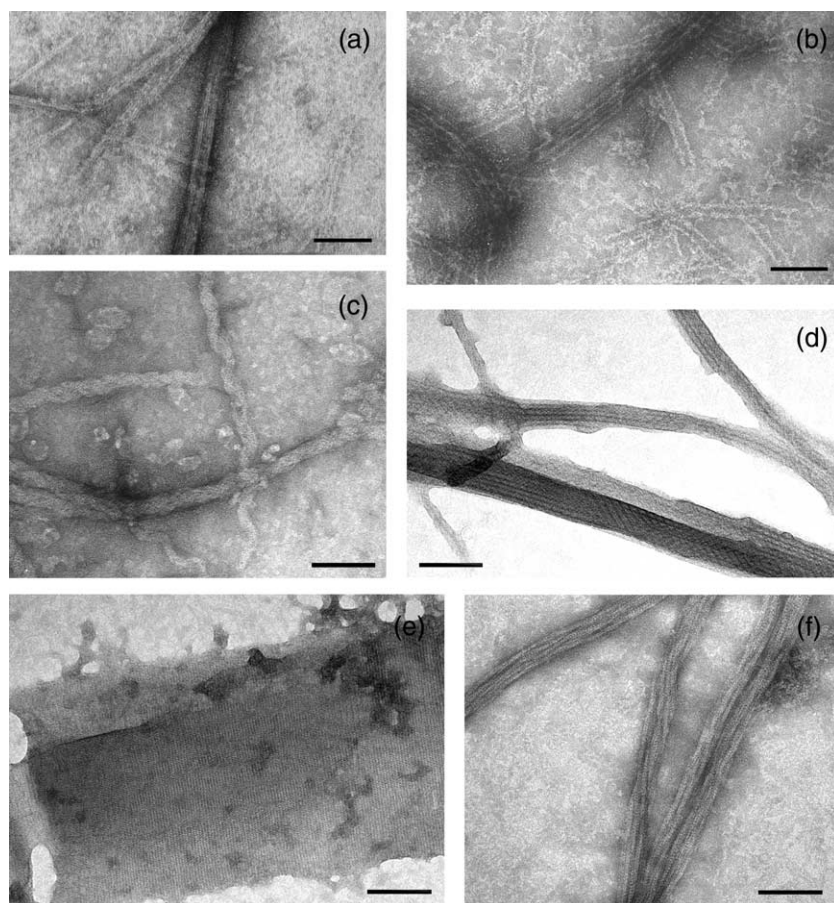


Figure 6. Polymers formed by FtsZ/tubulin chimeras. Polymers were generated at 55 °C in the presence of 50 mM Mes-KOH, 50 mM KCl, 1 mM EDTA, 6 mM MgCl₂, 1 mM GTP (pH 6.5). (a) Electron micrograph of negatively stained wild-type FtsZ polymers. (b) Electron micrograph of negatively stained polymers formed with FtsZ/T7 chimeras. (c) Electron micrograph of polymers formed with FtsZ/M chimeras. (d) and (e) Electron micrograph of polymers formed with FtsZ/T7M chimeras. (f) Electron micrograph of polymers formed with FtsZ/NT7M chimeras. Bars correspond to 100 nm.

polymers in the case of the FtsZ/T7M chimera (Figure 6(e)). These results are compatible with distortions of the lateral interactions between the FtsZ monomers in the double-stranded filament, generated by the inserted tubulin N and M-loops.

Discussion

In spite of their structural similarities, FtsZ and tubulin have important differences regarding their folding and polymerising behaviour. Whereas FtsZ does not appear to require the help of any chaperone to attain its native conformation,²⁰ tubulin needs the concourse of a number of chaperones to acquire a conformation able to generate the α,β -dimers that form the building blocks of the microtubules.^{3,4} The most important of the assisting chaperones is the cytosolic chaperonin CCT, whose interaction with tubulin is stringently required for the proper folding of the cytoskeletal protein.^{15,16,30} This interaction seems to occur through the apical domains of defined CCT subunits, and eight specific regions of tubulin located throughout its sequence.^{9,17} Most of these regions are not present in the prokaryotic homologue FtsZ, which does not interact with CCT *in vitro*,²⁸ and are also involved in the longitudinal and lateral contacts of the α,β -tubulin dimer that generate the protofilament and the microtubule, respectively.^{1,17,20} (Figure 1(a)). The loops that are involved in longitudinal contacts are the H3-S4 loop, located in the N-terminal region of tubulin (here called N-loop), the H7-H8 loop (T7-loop), the H8-S7 loop, the S9-S10 loop and the H11-H12 loop (in the very C-terminal region of tubulin). The loops that are involved in the lateral contacts are the H1-H2 loop, the H2-S3 loop, the S7-H9 loop (the M-loop) and also the N-loop. We have chosen three of these loops (the N, T7 and M-loop; Figure 1(a) and (b)) to determine whether they are able to induce in FtsZ any of the folding and polymerising properties of tubulin that seem to be associated with the presence of these loops.

The substitution of these loops does indeed alter the properties of FtsZ. In the case of the FtsZ/N chimera, the level of expression was very low, although the protein was expressed as a soluble protein. In the case of the FtsZ/NT7M chimera, although the level of expression is comparable to wild-type FtsZ, only half of the expressed protein is obtained in the soluble fraction. These results clearly suggest that the insertion of the N-loop alters the FtsZ stability, although in the case of the triple mutant as well as in the case of FtsZ/T7, FtsZ/M and FtsZ/T7M chimeras, the purified proteins have an average secondary structure similar to that of wild-type FtsZ, as observed by CD (Figure 2(a)). This suggests that the chimeras purified as soluble proteins are correctly folded, a notion that is reinforced by the fact that the mutants contain bound guanine nucleotide (see Materials and Methods) and are able to assemble (see

Results). It is, however, interesting to note that, when the relative intensity of the minima at 209 nm and 222 nm (the CD_{222}/CD_{209} ratio is an indication of the shape of the spectrum) is calculated for all the mutants measured, whereas the values obtained for the single mutants are more similar to that of wild-type FtsZ (FtsZ: 0.88; FtsZ/T7: 0.94; FtsZ/M: 0.90), the values obtained for the double and triple mutants resemble more that obtained for tubulin (FtsZ/T7M: 0.98; FtsZ/NT7M: 0.98; tubulin: 1.01). This may be compatible with the accumulation of inserted tubulin sequences changing the average secondary structure of FtsZ so that it resembles more that of tubulin. The unfolding/refolding experiments performed with four mutants reinforce this notion. Whereas, insertion of either the T7 or the M-loop causes a slight and reversible destabilisation of the unfolding process (Figure 2(b) and (c)), the accumulation of the two insertions in the FtsZ sequence generates a more complex, biphasic unfolding process that is still reversible (Figure 2(d)). However, the accumulation of the three tubulin sequences induces a biphasic unfolding profile very similar to that of tubulin (Figure 2(e) and (f)), which as in the case of the eukaryotic protein is irreversible, at least in the *in vitro* conditions used in these experiments. The discrepancy between the irreversibility of the unfolding process and the fact that part of the expressed FtsZ/NT7M mutant is able to attain its native conformation in *E. coli*, may be explained by the cytosolic environment (ionic and macromolecular crowding conditions) or by the presence of molecular chaperones in the prokaryote organism that help to overcome the folding problem of this FtsZ/tubulin triple mutant.

The changes in stability and folding behaviour of the FtsZ/tubulin chimeras are accompanied by changes in their ability to interact with the CCT. Whereas unfolded wild-type FtsZ is not able to bind to CCT (Figure 3), the insertion of any of the loops (N, T7 or M-loop) provides FtsZ with the ability to interact with the chaperonin (Figures 3–5). This occurs either when CCT is incubated with native FtsZ/tubulin chimeras or when the latter are chemically unfolded and the denaturant diluted in the presence of CCT. However, and based on the unfolding/refolding experiments described above, it is very likely that except in the case of FtsZ/NT7M, the unfolded chimeras reach their native conformation before interacting with CCT. In any case, it is an apparent paradox that the tubulin loops that induce the binding of the FtsZ/tubulin chimeras to CCT can only provide such interaction to the unfolded conformation of tubulin and not to the native one, and the only plausible explanation is that a possible sterical hindrance by the native structure of tubulin prevents the interaction of its CCT-binding loops with the apical domains of the cytosolic chaperonin.

It has been described previously that the interaction between unfolded tubulin and CCT is subunit-specific.⁹ The immunomicroscopy carried

out with complexes formed between CCT and FtsZ/tubulin chimeras, despite the large mass of the FtsZ molecule compared to the CCT cavity and the low resolution of this work, reinforce this notion. The insertion of the N-loop in the FtsZ/N chimera induces the binding of the FtsZ molecule to the apical domains of approximately the same CCT subunits which the N-terminal domain of unfolded tubulin interacts with (compare Figure 5(c) with (a), and Figure 5(d) with (b)). On the other hand, the insertion in the FtsZ sequence of the T7 and M-loops, located in the C-terminal domain of tubulin, induces the binding of the generated chimeras (FtsZ/T7, FtsZ/M and FtsZ/T7M) to approximately the same CCT subunits to which the C-terminal domain of tubulin interacts with (compare Figure 5(e), (g) and (i) with (a), and Figure 5(f), (h) and (j) with (b)). The interaction of the FtsZ/NT7M triple chimera with CCT is more complex, and can be explained by the fact that this mutant possesses CCT-binding domains of both the N and C-terminal domains of tubulin. However, in 70% of the CCT particles the FtsZ mass seems to interact with the CCT subunits involved in the interaction with the C-terminal domain of tubulin (Figure 5(k) and (l)) and in the remaining 30% the FtsZ mass seems to interact, approximately with the CCT subunits involved in the interaction with the N-terminal domain of tubulin (Figure 5(m) and (n)). This difference can be explained by the presence of two C-terminal CCT-binding domains (T7 and M-loop) compared to only one N-terminal CCT-binding domain (N-loop), and also by the fact that the M-loop is the strongest CCT-binder.^{9,17,18,26–28}

The inserted tubulin sequences seem also to induce in the FtsZ molecule new polymerising properties (Figure 6). Although more in-depth assembly studies were precluded by the limited solubility of FtsZ/tubulin chimeras under the assembly conditions required for FtsZ polymerisation, it is clear that the FtsZ/tubulin chimeras are capable of generating more complex polymeric structures than the double-stranded filaments observed for wild-type FtsZ²³ (Figure 6(a)). In particular, the insertion of the N and M-loops, involved in tubulin in the generation of the lateral contacts, induced the formation of curved polymers (Figure 6(c) and (d)).

In summary, the insertions in the sequence of FtsZ from *M. jannaschii* of some of the CCT-binding domains of tubulin introduce in the prokaryotic protein some properties that are unique to its eukaryotic homologue. Besides the ability of any of the FtsZ/tubulin chimeras to interact with the cytosolic chaperonin, the accumulation of these tubulin sequences in the FtsZ structure induces the conversion of the FtsZ/tubulin chimeras to a protein with a unfolding/refolding behaviour more similar to those of the eukaryotic protein.

It is generally believed that actin and tubulin are at the heart of the evolution of the eukaryotes³¹, providing these organisms with a more sophisticated cytoskeleton that is involved in important

processes such as cell division, chromosome segregation and segmentation, muscle contraction, amoeboid movement and processes of endocytosis and exocytosis, some of them unique to eukaryotes. It has also been suggested that CCT evolved to completion from a primitive chaperonin during the early stages of the evolution of eukaryotes,^{32,33} probably at the same time as tubulin.^{9,11,34} The finding that the largest differences between FtsZ and tubulin are located in the regions that in tubulin are involved in the interaction with CCT, and the fact that this chaperonin is stringently needed for the folding of the eukaryotic cytoskeletal protein, has prompted the suggestion that CCT may have co-evolved with tubulin to deal with the folding problems of the cytoskeletal protein.^{9,14,35} What are these folding problems? It seems clear that tubulin is able to acquire a large degree of folding without the need to bind to CCT, and a possible role of the interaction between CCT and tubulin could be the maintenance of a certain tubulin conformation necessary for the nucleotide loading that is so important in the stabilisation of the native conformation.^{9,36} Another possibility is the protection, through the interaction with CCT, of these regions that are involved in polymerisation, and that may be prone to unwanted interactions, a role in which other chaperones could also mediate.³ Although any of these hypotheses need to be tested, it is clear that accumulation of CCT-binding domains in the FtsZ sequence generates, besides the ability to interact with the cytosolic chaperonin, a molecule more similar to tubulin in its unfolding and refolding behaviour and its polymerising properties. These results doubtless strengthen the notion of a co-evolution of tubulin and the eukaryotic chaperonin.

Materials and Methods

Mutagenesis of FtsZ

Generation of mutant genes was carried out using the Quick Change site-directed mutagenesis kit of Stratagene. A pair of complementary oligonucleotide primers containing the desired mutation was designed for each mutant. PCR was performed using as template pHis17-MjFtsZ-H6 plasmid,²¹ which contains the wild-type FtsZ gene, and the complementary primers. After generation of the mutant plasmid, methylated DNA template was eliminated by digestion with DpnI. Competent *E. coli* XL1blue cells were transformed with PCR-DNA and clones obtained were subjected to restriction analysis and DNA sequencing. Five different FtsZ/tubulin chimeras were generated: the FtsZ/N chimera had the *M. jannaschii* FtsZ sequence of the N loop (placed between H3 and S4) switched by the corresponding sequence of mouse β 2-tubulin, the FtsZ/T7 chimera had the FtsZ sequence of the T7 loop (placed between H7 and H8) switched by the corresponding β -tubulin sequence, the FtsZ/M chimera had the FtsZ sequence of the M loop (placed between S7 and H9) switched by the corresponding β -tubulin sequence, the FtsZ/T7M double chimera was generated by the combined mutations of FtsZ/T7 and FtsZ/M

chimeras, and the FtsZ/NT7M triple chimera was generated by the combined mutations of FtsZ/N, FtsZ/T7 and FtsZ/M chimeras. The FtsZ/N chimera was generated by switching the FtsZ sequence SD by the corresponding β -tubulin sequence of SESCDCLQ and for that, primers CAATACAAGATTTCAGAAAGCTGCGATTGC CTGAGATGGTATTTATTAC and GTAATAAATACCATCTGC AGGCAATCGCAGCTTTCTGAATCTTGATTG were used. The FtsZ/T7 chimera was generated by switching the FtsZ sequence VELITKDGLINVDFA by the corresponding β -tubulin sequence TTCLRFPGQLNADLRK. Because this mutation involved the change of 16 amino acid residues and in order to design primers shorter than 30 nucleotides, the mutation was carried out in two steps. In a first step, the first eight amino acid residues were changed using primers GCTGTAAAGGGATTAACAT GCTTAAGATTCCCTGGATTGATTAATG and CATTATCAAT CCAGGGAATCTTAAGCATGTAGTTAATCCCTTTACAGC. In a second step, the remaining eight amino acid residues were substituted by using primers GATTCCCTGGACAG CTTAATGCTGATTTCGCTAAAGTTAAAGCTGTTA and TAAC AGCTTTAACTTTACGCAAATCAGCATTAAGCTGTCCAGGG AATC. The FtsZ/M chimera was generated by switching the FtsZ sequence SEKRAKE by the corresponding β -tubulin sequence SRGSQQYRALTVPE. This mutation was also carried out in two steps: first, the introduction of a unique SacII site and the elimination of EKRAK coding sequence, using the primers GGAGAGTGATAGCCGCGTT AGTATGGC and GCCATACTAACC GCGCTATCACTCTCC, and second the cloning and insertion into the SacII site of the SRGSQQYRALTVK coding sequence using the primers GGAAGCCAGCAGTATCGTGCGCTGACCGTGCCGG AAGC and TTCCGGCAGCGTCAGCGCACGATACTGCTGG CTTCCGC. The double chimera FtsZ/T7M was generated by inserting the T7 loop as described above in the plasmid containing the FtsZ/M chimera gene (pHis17-M loop). The triple chimera FtsZ/NT7M was generated replacing the NdeI/EcoRV fragment (438 bp long) of the pHis17-T7M loop plasmid (containing the double chimera FtsZ/MT7) with the same fragment of pHis17-N loop plasmid, which contains the mutation of the FtsZ/N chimera.

Protein expression, purification and concentration measurements

FtsZ from *M. jannaschii* and the FtsZ/ β -tubulin chimeras FtsZ/N, FtsZ/T7, FtsZ/M, FtsZ/T7M and FtsZ/NT7M, all with a C-terminal His tag, were over-produced in *E. coli* BL21 (DE3) pLys, purified as described for FtsZ,²⁰ and stored concentrated at -80°C . Their guanine nucleotide content and protein concentration were determined by cold 0.5 N HClO₄ extraction and spectrophotometric measurements as described.²⁰ The extinction coefficients employed for the apoproteins in 6 M GdmCl were $\epsilon_{280}=6970\text{ M}^{-1}\text{ cm}^{-1}$ and $\epsilon_{254}=4224\text{ M}^{-1}\text{ cm}^{-1}$ (calculated for 1Trp, 1Tyr and 8Phe in FtsZ and FtsZ/T7), or $\epsilon_{280}=8250\text{ M}^{-1}\text{ cm}^{-1}$ and $\epsilon_{254}=4533\text{ M}^{-1}\text{ cm}^{-1}$ (calculated for 1Trp, 2Tyr and 8Phe in FtsZ/M, FtsZ/T7M and FtsZ/NT7M). The purified FtsZ/tubulin chimera contained 0.6–0.9 guanosine nucleotide bound, similarly to FtsZ.^{20,23}

CCT was purified from soluble extracts of bovine testis as described.³⁷ The CCT:FtsZ complexes (either with wild-type or FtsZ/tubulin chimeras) were formed by incubating CCT and the FtsZ proteins in a 1 : 10 molar ratio for 30 minutes at 25°C . In the case of the CCT:FtsZ:antibody immunocomplexes, preformed CCT:FtsZ complexes were incubated with anti-CCT δ 8 g

monoclonal antibody (Stressgene; 5 : 1 antibody:complex molar ratio) during 15 minutes at room temperature.

Circular dichroism and protein unfolding

CD spectra and measurements were recorded in a JASCO 720-715 spectropolarimeter, employing respectively 0.1 mm and 1 mm cells in a thermostated cell holder at 25°C .²⁰ Solutions of GdmCl were prepared gravimetrically and their concentration was confirmed by refractometry as described.³⁸ Proteins were first diluted to 8 mg/ml in 20 mM Pipes-KOH (pH 7.5), 5 mM DTT for the unfolding curve. For the refolding curve, they were prepared in the same buffer containing 6 M GdmCl and held a minimum 30 minutes at 25°C . In both cases they were carefully diluted into different GdmCl concentrations (0–5 M) (final protein concentration 0.16 mg/ml). After incubation for 48 hours at 25°C in order to reach equilibrium, the CD of each sample at 222 nm was measured during ten minutes.

CCT binding assays

Substrate-free CCT was incubated for 30 minutes at 25°C with excess (10 : 1 mol:mol) of either native or 6 M GdmCl denatured tubulin, FtsZ and the various FtsZ mutants. The incubation with CCT was such that the GdmCl concentration was decreased to 100 mM. The samples were subjected to a native electrophoresis using 4% acrylamide gels run at 90–100 V for 2–3 hours. This allowed a complete separation of the CCT band, which carried the bound substrates, from that of the substrate not bound to the chaperonin. The gels were stained with Bio-Safe[™] Coomassie (BIO-RAD) and the CCT bands were subsequently excised, dehydrated at 90°C for ten minutes and rehydrated with a denaturing loading electrophoresis buffer. Samples were boiled for ten minutes and loaded onto a SDS electrophoresis gel. Alternatively, when immunoblotting was performed, bands from the SDS gels were transferred overnight (4°C and 90 mA current) to a 0.2 μm nitrocellulose membrane (BIO-RAD) using a Hoefer[®] TE Series Transphor Electrophoresis Unit. The nitrocellulose membrane was subsequently blocked by washing the membrane with WB buffer (3% skimmed milk, 0.05% Tween-20 in PBS buffer) for two hours at room temperature. The membrane was then incubated with the first antibody (diluted between 1 : 1000 and 1 : 2000 in WB buffer) for one hour at 37°C with gentle agitation. The membrane was washed several times with WB buffer and then subjected to a treatment with the peroxidase conjugated rabbit anti-mouse secondary antibody (Dakopatts; diluted 1 : 2000 in WB buffer) for 30 minutes at 37°C . The membrane was again washed several times with WB buffer at room temperature and subsequently developed with ECL[®] Plus Western Blotting Detection System (Amersham Biosciences[®]). An antibody against the His-tag present in all the FtsZ sequences (Amersham) was used to determine the presence of FtsZ, and DM1B antibody against β -tubulin (Amersham) was used in the case of tubulin

FtsZ assembly and electron microscopy

FtsZ assembly was monitored by electron microscopy as described,²³ with several modifications. Proteins were diluted to 0.5 mg/ml into assembly buffer (50 mM Mes-KOH, 50 mM KCl, 1 mM EDTA, pH 6.5) at 55°C (the His-tagged FtsZ and FtsZ/tubulin chimeras have a

marked tendency to precipitate at pH 6.5 in the cold) and centrifuged at 100,000 g during ten minutes in a pre-warmed Beckman TL100 rotor to eliminate any aggregate. Assembly was started by addition of 1 mM GTP and 6 mM MgCl₂ at 55 °C. After two minutes, samples were adsorbed to formvar and carbon-coated grids on a hot plate (one minute), and stained at room temperature with 2% uranyl acetate (30 seconds). Images were taken at different magnifications in a JEOL 1230 microscope operated at 100 KV. In the case of the CCT:FtsZ complexes or in the CCT:FtsZ:antibody immunocomplexes, 5 µl aliquots were applied to glow-discharged carbon grids for one minute and then stained for one minute with 2% uranyl acetate. Images were recorded at 0°-tilt in a JEOL 1200EX-II electron microscope operated at 100 KV and recorded on Kodak SO-163 film at 60,000× nominal magnification.

Image processing and two-dimensional averaging

Micrographs for image processing were digitised in a Zeiss SCAI scanner with a sampling window corresponding to 3.5 Å/pixel for negatively-stained specimens. For two-dimensional classification and averaging, particles of the CCT:FtsZ complexes and immunocomplexes were selected, aligned using a free-pattern algorithm³⁹ and classified using self-organising maps.⁴⁰

Acknowledgements

This work was supported by grants BMC 2001-0950 and BFU2004-00232 to J.M.V., BMC 2002-00996 to J.L.C. and BIO 2002-03665 to J.M.A. We are grateful to Dr Gómez-Puertas for his help with Figure 1.

References

- Nogales, E. (2000). Structural insights into microtubule function. *Annu. Rev. Biochem.* **69**, 277–302.
- Jenkins, C., Samudrala, R., Anderson, I., Hedlund, B. P., Petroni, G., Michailova, N. *et al.* (2002). Genes for the cytoskeletal protein tubulin in the bacterial genus *Prostheobacter*. *Proc. Natl Acad. Sci. USA*, **99**, 17049–17056.
- López-Fanarraga, M., Avila, J., Guasch, A., Coll, M. & Zabala, J. C. (2001). Postchaperonin tubulin folding cofactors and their role in microtubule dynamics. *J. Struct. Biol.* **135**, 219–229.
- Cowan, N. J. & Lewis, S. A. (2002). Type II chaperonins, prefoldin and the tubulin-specific chaperones. *Advan. Protein Chem.* **59**, 73–104.
- Lewis, V. A., Hynes, G. M., Zheng, D., Saibil, H. & Willison, K. (1992). T-complex polypeptide-1 is a subunit of a heteromeric particle in the eukaryotic cytosol [see comments]. *Nature*, **358**, 249–252.
- Gao, Y., Thomas, J. O., Chow, R. L., Lee, G. H. & Cowan, N. J. (1992). A cytoplasmic chaperonin that catalyzes beta-actin folding. *Cell*, **69**, 1043–1050.
- Frydman, J., Nimmesgern, E., Erdjument-Bromage, H., Wall, J. S., Tempst, P. & Hartl, F. U. (1992). Function in protein folding of TRiC, a cytosolic ring complex containing TCP-1 and structurally related subunits. *EMBO J.* **11**, 4767–4778.
- Llorca, O., Smyth, M. G., Carrascosa, J. L., Willison, K. R., Radermacher, M., Steinbacher, S. & Valpuesta, J. M. (1999). 3D reconstruction of the ATP-bound form of CCT reveals the asymmetric folding conformation of a type II chaperonin. *Nature Struct. Biol.* **6**, 639–642.
- Llorca, O., Martin-Benito, J., Ritco-Vonsovici, M., Grantham, J., Hynes, G. M., Willison, K. R. *et al.* (2000). Eukaryotic chaperonin CCT stabilizes actin and tubulin folding intermediates in open quasi-native conformations. *EMBO J.* **19**, 5971–5979.
- Liou, A. K. & Willison, K. R. (1997). Elucidation of the subunit orientation in CCT (chaperonin containing TCP1) from the subunit composition of CCT microcomplexes. *EMBO J.* **16**, 4311–4316.
- Willison, K. R. (1999). In *Molecular Chaperones and Folding Catalysts* (Bukau, B., ed.), pp. 555–571, Harwood Academic Publishers, Amsterdam.
- Gómez-Puertas, P., Martín-Benito, J., Carrascosa, J. L., Willison, K. R. & Valpuesta, J. M. (2004). The substrate recognition mechanisms in chaperonins. *J. Mol. Recog.* **17**, 85–94.
- Valpuesta, J. M., Carrascosa, J. L. & Willison, K. R. (2005). Structure and Function of the Cytosolic Chaperonin CCT. In *Protein Folding Handbook* (Butcher, J. & Kiefhaber, T., eds). Wiley-VCH, Weinheim, pp. 725–755.
- Llorca, O., Martin-Benito, J., Grantham, J., Ritco-Vonsovici, M., Willison, K. R., Carrascosa, J. L. & Valpuesta, J. M. (2001). The “sequential allosteric ring” mechanism in the eukaryotic chaperonin-assisted folding of actin and tubulin. *EMBO J.* **20**, 4065–4075.
- Sternlicht, H., Farr, G. W., Sternlicht, M. L., Driscoll, J. K., Willison, K. & Yaffe, M. B. (1993). The t-complex polypeptide 1 complex is a chaperonin for tubulin and actin *in vivo*. *Proc. Natl Acad. Sci. USA*, **90**, 9422–9426.
- Chen, X., Sullivan, D. S. & Huffaker, T. C. (1993). Two yeast genes with similarity to TCP-1 are required for microtubule and actin function *in vivo*. *Proc. Natl Acad. Sci. USA*, **91**, 9111–9115.
- Llorca, O., Martin-Benito, J., Gomez-Puertas, P., Ritco-Vonsovici, M., Willison, K. R., Carrascosa, J. L. & Valpuesta, J. M. (2001). Analysis of the interaction between the eukaryotic chaperonin cct and its substrates actin and tubulin. *J. Struct. Biol.* **135**, 205–218.
- Ritco-Vonsovici, M. & Willison, K. R. (2000). Defining the eukaryotic chaperonin-binding sites in human tubulins. *J. Mol. Biol.* **304**, 81–98.
- Nogales, E., Whittaker, M., Milligan, R. A. & Downing, K. H. (1999). High-resolution model of the microtubule. *Cell*, **96**, 79–88.
- Andreu, J. M., Oliva, M. A. & Monasterio, O. (2002). Reversible unfolding of FtsZ cell division proteins from archaea and bacteria. Comparison with eukaryotic tubulin folding and assembly. *J. Biol. Chem.* **277**, 43262–43270.
- Löwe, J. & Amos, L. A. (1998). Crystal structure of the bacterial cell-division protein FtsZ complexed with GDP. *Nature*, **391**, 203–206.
- Bi, E. F. & Lutkenhaus, J. (1991). FtsZ ring structure associated with division in *Escherichia coli*. *Nature*, **353**, 161–164.
- Oliva, M. A., Huecas, S., Palacios, J. M., Martin-Benito, J., Valpuesta, J. M. & Andreu, J. M. (2003). Assembly of archaeal cell division protein FtsZ and a GTPase-inactive mutant into double-stranded filaments. *J. Biol. Chem.* **278**, 33562–33570.

24. Nogales, E., Wolf, S. G. & Downing, K. H. (1998). Structure of the $\alpha\beta$ tubulin dimer by electron crystallography. *Nature*, **391**, 199–203.
25. Löwe, J. & Amos, L. A. (1999). Tubulin-like protofilaments in Ca^{2+} -induced FtsZ sheets. *EMBO J.* **18**, 2364–2371.
26. Dobrzynski, J. K., Sternlicht, M. L., Farr, G. W. & Sternlicht, H. (1996). Newly-synthesized β -tubulin demonstrates domain-specific interactions with the cytosolic chaperonin. *Biochemistry*, **35**, 15870–15882.
27. Rommelaere, H., de Neve, M., Melki, R., Vandekerckhove, J. & Ampe, C. (1999). The cytosolic class II chaperonin CCT recognizes delineated hydrophobic sequences in its target proteins. *Biochemistry*, **38**, 3246–3257.
28. Dobrzynski, J. K., Sternlicht, M. L., Peng, I., Farr, G. W. & Sternlicht, H. (2000). Evidence that β -tubulin induces a conformation change in the cytosolic chaperonin which stabilizes binding: implications for the mechanism of action. *Biochemistry*, **39**, 3988–4003.
29. Llorca, O., McCormack, E. A., Hynes, G., Grantham, J., Cordell, J., Carrascosa, J. L. *et al.* (1999). Eukaryotic type II chaperonin CCT interacts with actin through specific subunits. *Nature*, **402**, 693–696.
30. Úrsic, D. & Culbertson, M. R. (1991). The yeast homolog to mouse Tcp-1 affects microtubule-mediated processes. *Mol. Cell. Biol.* **11**, 2629–2640.
31. Doolittle, R. F. (1995). The origins and evolution of eukaryotic proteins. *Phil. Trans. Roy. Soc. London B*, **349**, 235–240.
32. Kubota, H., Hynes, G., Carne, A., Asworth, A. & Willison, K. (1994). Identification of six TCP-1 related genes encoding divergent subunits of the TCP-1 containing chaperonin. *Curr. Biol.* **4**, 89–99.
33. Kubota, H., Hynes, G. & Willison, K. (1995). The chaperonin containing t-complex polypeptide 1 (TCP-1). Multisubunits machinery assisting in protein folding and assembly in the eukaryotic cytosol. *Eur. J. Biochem.* **230**, 3–16.
34. Willison, K. R. & Horwich, A. L. (1996). In *The Chaperonins* (Ellis, R. J., ed.), pp. 107–135, Academic Press.
35. Archibald, J. M., Blouin, C. & Ford Doolittle, W. (2001). Gene duplication and the evolution of group II chaperonins: implications for structure and function. *J. Struct. Biol.* **135**, 157–169.
36. Tian, G., Vainberg, I. E., Tap, W. D., Lewis, S. A. & Cowan, N. J. (1995). Quasi-native chaperonin-bound intermediates in facilitated protein folding. *J. Biol. Chem.* **270**, 23910–23913.
37. Martín-Benito, J., Boskovic, J., Gómez-Puertas, P., Carrascosa, J. L., Simons, C., Lewis, S. A. *et al.* (2002). Structure of eukaryotic prefoldin and of its complexes with unfolded actin and the cytosolic chaperonin CCT. *EMBO J.* **21**, 6377–6386.
38. Pace, C. N. & Scholtz, J. M. (1997). In *Protein Structure: A Practical Approach* (Creighton, T. E., ed.) 2nd edit., pp. 299–321, Oxford University Press, Oxford.
39. Marco, S., Chagoyen, M., de la Fraga, L. G., Carazo, J. M. & Carrascosa, J. L. (1996). A variant to the “random approximation” of the reference-free alignment. *Ultramicroscopy*, **66**, 5–10.
40. Marabini, R. & Carazo, J. M. (1994). Pattern recognition and classification of images of biological macromolecules using artificial neural networks. *Biophys. J.* **66**, 1804–1814.
41. Wang, D., Villasante, A., Lewis, S. A. & Cowan, N. J. (1986). The mammalian β -tubulin repertoire: hematopoietic expression of a novel, heterologous β -tubulin sequence. *J. Cell. Biol.* **103**, 1903–1910.

Edited by W. Baumeister

(Received 29 July 2004; received in revised form 11 November 2004; accepted 17 November 2004)